Supplementary materials

A Smart Nanocomposite System for Controlled Insulin Release and Glucose Sensing in Diabetes Management

Dan Wang[a, #], Yaoyao Wang[a, #], Wilson Dumisani Gamuchirai Dube[a, #], Jiarong Zhang[a], Jie Gao[a], Xue Tang[a], Gisèle Ineza Urujeni[a], Yajie Zhang[a], Linjie Zhao[a], Hua He[a, b, c], Deli Xiao[a, b, c*], Pierre Dramou[a, b, c*]

a Department of Analytical Chemistry, China Pharmaceutical University, Nanjing 210009, China.

b Key Laboratory of Drug Quality Control and Pharmacovigilance (China Pharmaceutical University), Ministry of Education, 24 Tongjia Lane, Nanjing 210009, China

c Key Laboratory of Biomedical Functional Materials, China Pharmaceutical University, Nanjing 210009, China

Corresponding Authors:

* To whom correspondence should be addressed:

China Pharmaceutical University, 639 Longmian Avenue, Nanjing 211198, Jiangsu Province, China.

E-mail addresses: pierred@cpu.edu.cn; dpl_a505@163.com (P. Dramou)

xiao49562001@163.com (D. Xiao)

#: Dan Wang, Yaoyao Wang and Wilson Dumisani Gamuchirai Dube contributed equally to this work and should be considered co-first authors.

Table of Contents

Conditions of HPLC:

The release of insulin was quantified using High-Performance Liquid Chromatography (HPLC, LC-20AT, Shimadzu, Japan) with an SPD-M20A UV detector. The model of the column was C18 that is 250 mm × 4.6 mm id, 5.0 μm from Shimadzu, and the temperature of column heater was maintained at 30 °C. The mobile phase was composed of ultrapure water (phase A) and acetonitrile (phase B). The gradient elution began with 60% phase B, which was maintained for 2 min to allow for initial equilibration. After this period, the concentration of phase B was gradually increased to 70% over the course of 8 min and kept for 2 min. Finally, the concentration of phase B was decreased back to 60% over 3 min, returning to the initial conditions to stabilize the system for the next run. The acetonitrile and water were consisted for mobile phase, with a flow rate of 1.0 mL min^{-1}. The HPLC method was validated for accuracy, precision, and recovery using standard insulin solutions.

Control experiments using ZIF-8@Ins-AuNCs (without GOx) were performed to validate that the observed release was due to glucose oxidation.

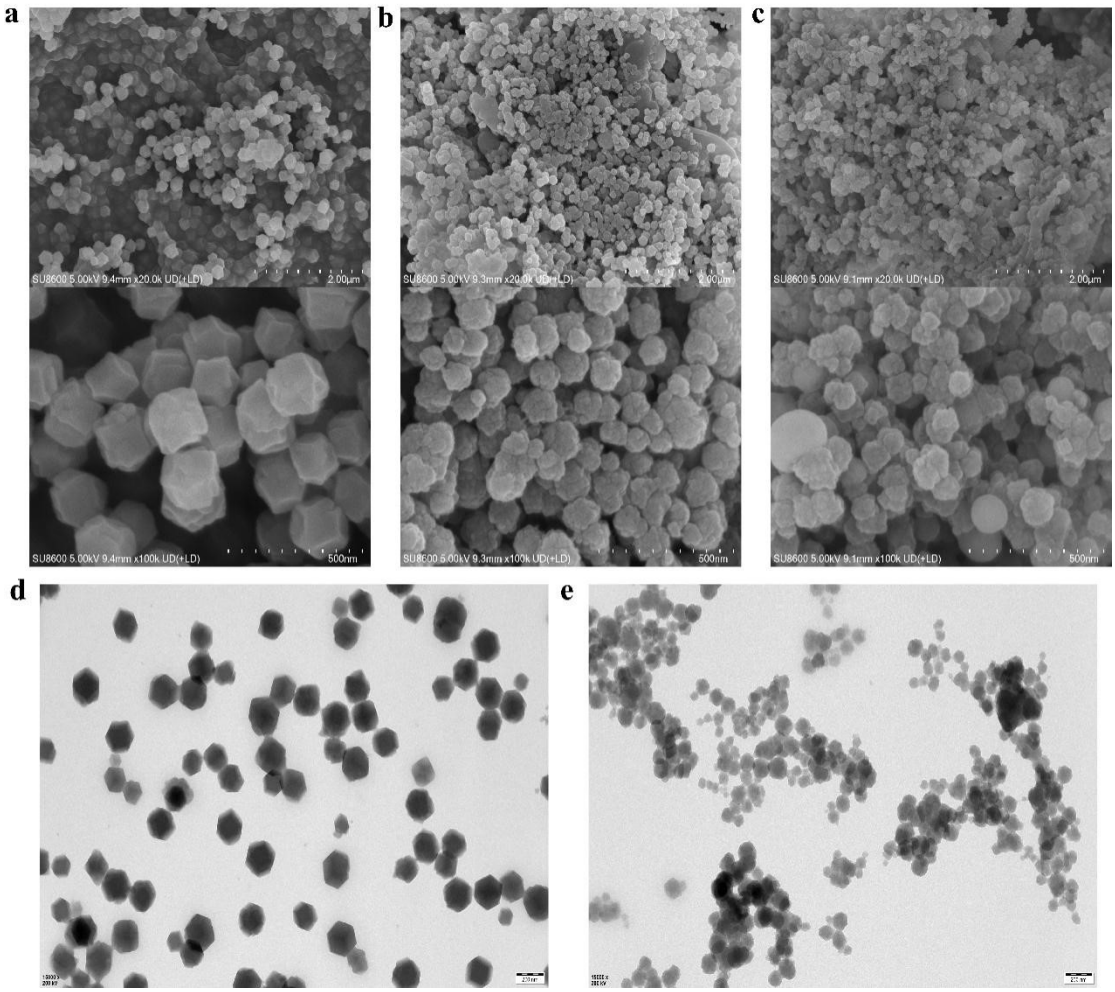

Supplementary Figure 1. Characterization of ZIF-8 and ZIF-8@Ins-GOx/AuNCs. **a**, SEM images of ZIF-8 showing its typical morphology. **b**, SEM images of ZIF-8@Ins-GOx/AuNCs demonstrating the successful integration of AuNCs within the ZIF-8 framework. **c**, SEM images of ZIF-8@Ins-GOx/AuNCs reacted with glucose, illustrating structural changes after glucose interaction. **d**, TEM image of ZIF-8, highlighting its surface structure. **e**, TEM image of ZIF-8@Ins-GOx/AuNCs, showing the surface characteristics after AuNCs and insulin incorporation.

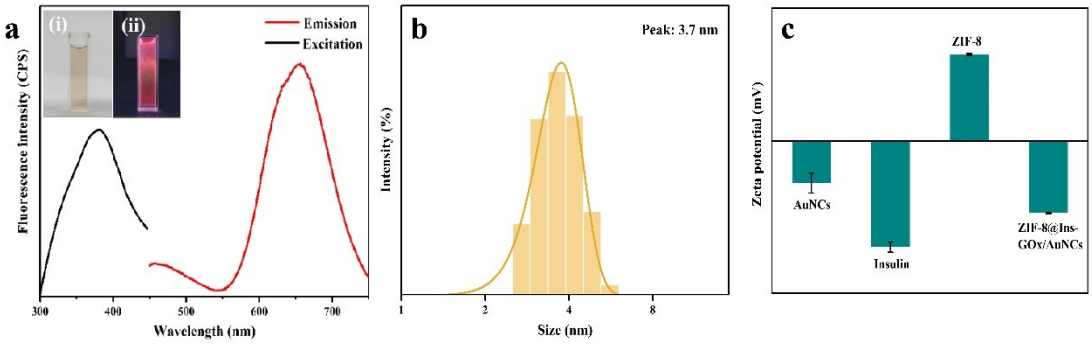

Supplementary Figure 2. Characterization of AuNCs. a, The fluorescence excitation and emission spectra of AuNCs. Inset images display the AuNCs solution under visible light (i) and under a UV lamp (365 nm) (ii). **b,** The size distribution of AuNCs. **c,** Zeta potential values for AuNCs, Insulin, ZIF-8, and ZIF-8@Ins-GOx/AuNCs nanocomposites.

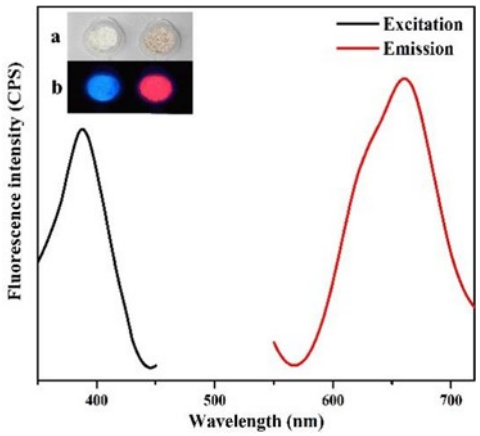

Supplementary Figure 3. Excitation and emission spectra of ZIF-8@Ins-GOx/AuNCs. Excitation and emission spectra of ZIF-8@Ins-GOx/AuNCs are shown. Inset images display ZIF-8 (left) and ZIF-8@Ins-GOx/AuNCs (right) under visible light (a) and UV lamp (b).

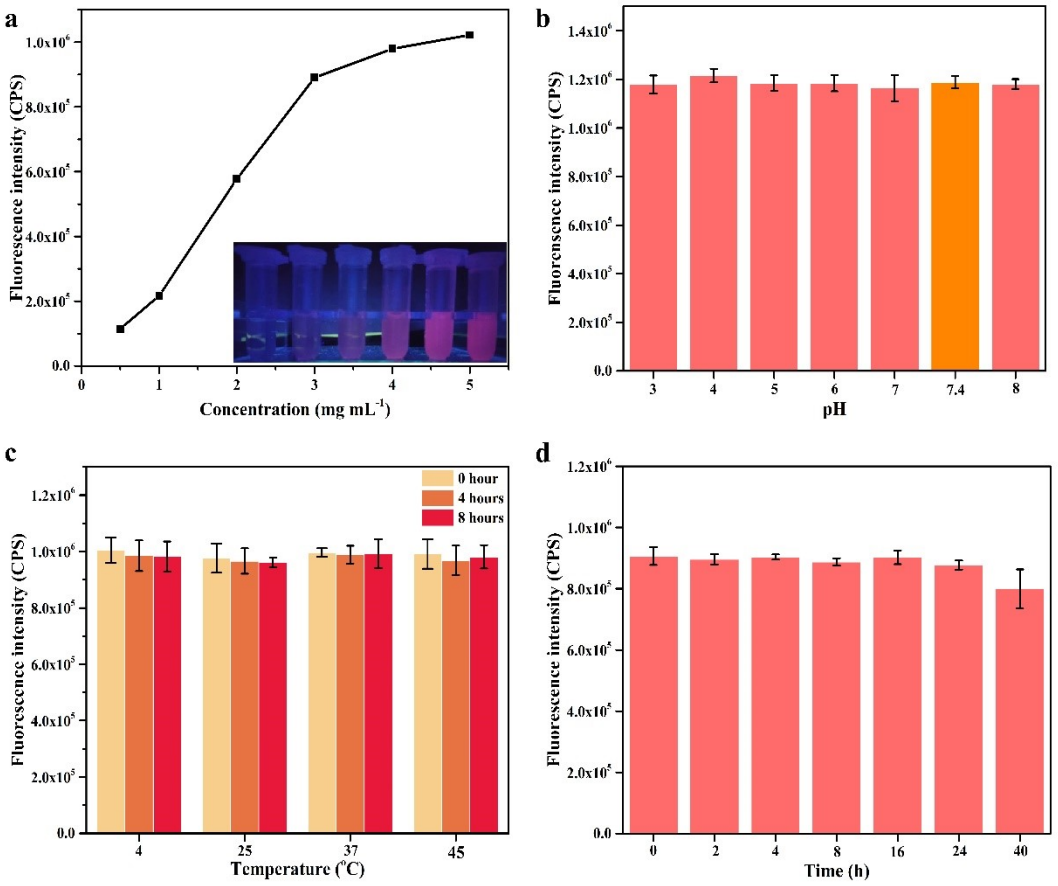

Supplementary Figure 4. Optimization and Stability of Fluorescent Systems. a, concentration investigation of ZIF-8@Ins-GOx/AuNCs. **b**, The pH stability of ZIF-8@Ins-GOx/AuNCs in the range of 3.0~8.0. **c**, The temperature stability of ZIF-8@Ins-GOx/AuNCs (4~45 °C). **d**, The study of photobleaching resistance.

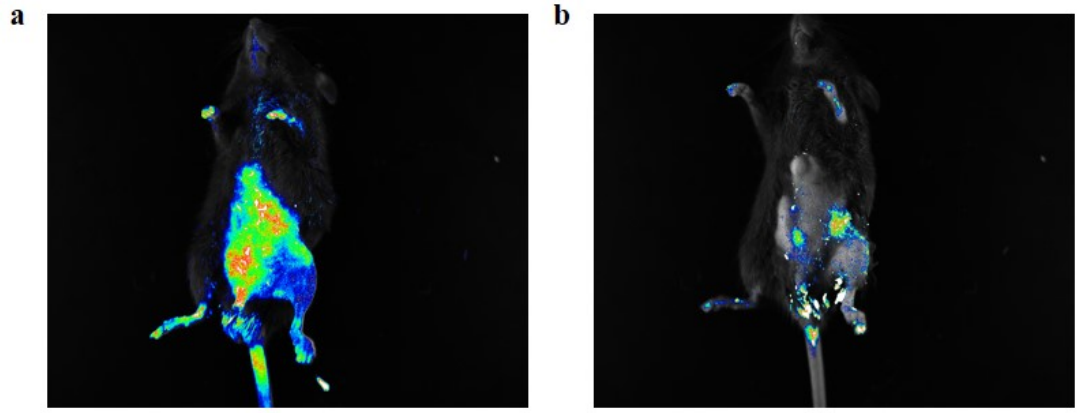

Supplementary Figure 5. Images of mice taken under a fluorescence imager after

intraperitoneal injection of ZIF-8@Ins-GOx/AuNCs. Mouse with normal blood glucose levels (**a**) and mouse with high blood glucose levels (**b**).

Supplementary Table 1. The pore of ZIF-8 and ZIF-8@Ins-GOx/AuNCs

Materials	BET Surface Area (m^2 g^{-1})	Pore Volume (cm^3 g^{-1})
ZIF-8	1427.1336	0.682577
ZIF-8@Ins-GOx/AuNCs	823.9545	0.636925

Supplementary Table 2. Linear range, limit of detection and quantification of glucose.

Sample	Linear range (mM)	Linear relationship	R^2	LOD (mM)	LOQ (mM)
Glucose	2.50 - 200	y=-2395x+867000	0.9976	0.80	2.41

Supplementary Table 3. Recovery rate of glucose after spiking with standard solution (n = 5).

Sample	Added (mM)	Detected (mM)	Recovery	RSD (%)
Bovine serum	50	50.69	101.39	2.88
	100	99.19	99.19	1.28
	120	117.00	97.53	0.54

Supplementary Table 4. Linear range, limit of detection and quantification of insulin.

Sample	Linear range (mg mL^{-1})	Linear relationship	R^2	LOD (mg mL^{-1})	LOQ (mg mL^{-1})
Insulin	0.001 - 1.0	y=9.515E6x+42300	0.9978	0.00010	0.00015

Supplementary Table 5. Recovery rate of insulin after spiking with standard solution (n=6).

Sample	Concentration	Intra-day precision		Inter-day precision	
	(mg mL^{-1})	Recovery	RSD (%)	Recovery	RSD (%)
Insulin	0.07	97.65	0.13	97.33	0.16
	0.25	99.27	0.14	99.45	0.13
	0.50	99.48	0.11	99.78	0.18